

Cite this: *Food Funct.*, 2023, 14, 4163

## Improving endothelial health with food-derived H<sub>2</sub>S donors: an *in vitro* study with S-allyl cysteine and with a black-garlic extract enriched in sulfur-containing compounds†

Federica Geddo,<sup>a</sup> Giulia Querio,<sup>a</sup> Alberto Asteggiano,<sup>b,c</sup> Susanna Antoniotti,<sup>a</sup> Alessandra Porcu,<sup>d</sup> Andrea Occhipinti,<sup>d</sup> Claudio Medana<sup>b</sup> and Maria Pia Gallo<sup>\*,a</sup>

A healthy vascular endothelium plays an essential role in modulating vascular tone by producing and releasing vasoactive factors such as nitric oxide (NO). Endothelial dysfunction (ED), the loss of the endothelium physiological functions, results in the inability to properly regulate vascular tone, leading to hypertension and other cardiovascular risk factors. Alongside NO, the gasotransmitter hydrogen sulfide (H<sub>2</sub>S) has emerged as a key molecule with vasodilatory and antioxidant activities. Since a reduction in H<sub>2</sub>S bioavailability is related to ED pathogenesis, natural H<sub>2</sub>S donors are very attractive. In particular, we focused on the sulfur-containing amino acid S-allyl cysteine (SAC), a bioactive metabolite, of which black garlic is particularly rich, with antioxidant activity and, among others, anti-diabetic and anti-hypertensive properties. In this study, we analyzed the protective effect of SAC against ED by evaluating reactive oxygen species level, H<sub>2</sub>S release, eNOS phosphorylation, and NO production (by fluorescence imaging and western blot analysis) in Bovine Aortic Endothelial cells (BAE-1). Furthermore, we chemically characterized a Black Garlic Extract (BGE) for its content in SAC and other sulfur-containing amino acids. BGE was used to carry out an analysis on H<sub>2</sub>S release on BAE-1 cells. Our results show that both SAC and BGE significantly increase H<sub>2</sub>S release. Moreover, SAC reduces ROS production and enhances eNOS phosphorylation and the consequent NO release in our cellular model. In this scenario, a natural extract enriched in SAC could represent a novel therapeutic approach to prevent the onset of ED-related diseases.

Received 31st January 2023,  
Accepted 7th April 2023

DOI: 10.1039/d3fo00412k

rsc.li/food-function

## Introduction

The vascular endothelium is a monolayer of specialized cells that lines the inside of the circulatory system and is a key regulator of vascular homeostasis. In particular, the endothelial cells represent the interface between blood and both the vascular wall and the tissue interstitium, managing and mediating the effects of circulating molecules on the smooth muscle layer. Within this role, a healthy endothelium produces and releases itself vasoactive factors such as nitric oxide (NO) and other endothelium-dependent hyperpolarizing factors which

maintain adequate vascular tone and blood fluidity, and promotes antioxidant and anti-inflammatory effects.<sup>1,2</sup>

Endothelial dysfunction (ED) refers to a systemic condition characterized by the loss of these physiological functions caused by different risk factors, including dyslipidemia, diabetes mellitus, and aging.<sup>3</sup> This turns out in the inability of the endothelium to properly regulate vascular tone, due to the reduction of NO production, which is associated with the impairment of vascular smooth muscle relaxation and hypertension.

Besides NO, the endogenous gasotransmitter hydrogen sulfide (H<sub>2</sub>S) is emerging as an essential molecule involved in the regulation of the cardiovascular system, by affecting vascular smooth muscle cells, endothelial cells, and perivascular nerves,<sup>4</sup> in a strictly crosstalk with the NO-pathway. In mammalian species, H<sub>2</sub>S is mostly enzymatically produced by three enzymes in the cysteine biosynthesis pathway, including cystathionine-β-synthase (CBS), cystathionine-γ-lyase (CSE), and 3-mercaptopyruvate sulfurtransferase (3-MST), while only a small part is produced by non-enzymatic pathways.<sup>5</sup> H<sub>2</sub>S main physiological effects on the vasculature includes vasorelaxation and antioxidant/anti-inflammatory activities,<sup>2</sup> whose

<sup>a</sup>Department of Life Sciences and Systems Biology, University of Turin, Via Accademia Albertina 13, 10123 Turin, Italy. E-mail: mariapia.gallo@unito.it

<sup>b</sup>Molecular Biotechnology and Health Sciences Department, Università degli Studi di Torino, Via Pietro Giuria 5, 10125 Torino, Italy

<sup>c</sup>Biosfered S.r.l., Via Paolo Veronese 202, 10148 Torino, Italy

<sup>d</sup>Abel Nutraceuticals S.r.l., Via Paolo Veronese 202, 10148 Torino, Italy

† Electronic supplementary information (ESI) available. See DOI: <https://doi.org/10.1039/d3fo00412k>



molecular mechanisms are related to H<sub>2</sub>S-dependent S-sulphydration of proteins and redox reactions. Indeed, a reduction in H<sub>2</sub>S bioavailability is related to the pathogenesis of ED and leads to a series of cardiovascular disorders, such as atherosclerosis and hypertension.<sup>6</sup> Moreover, H<sub>2</sub>S has recently emerged as an inhibitor of the sympathetic outflow, even if results on this point are still debated.<sup>7</sup>

In this scenario, H<sub>2</sub>S donors derived from natural sources could represent a novel therapeutic strategy for preventing the onset of ED-related diseases. Among these, garlic (*Allium sativum*) is well-known for its cardioprotective effects.<sup>8</sup> In particular, S-allyl cysteine (SAC) is one of the most abundant bioactive compounds derived from aged garlic which is used as a dietary supplement and in traditional medicine; it is considered an H<sub>2</sub>S-producing agent<sup>9</sup> and possesses high antioxidant and anti-inflammatory activities.<sup>10–12</sup> Moreover, SAC exerts multiple healthy properties, such as anti-diabetic,<sup>13,14</sup> anti-cancer,<sup>15</sup> anti-hepatotoxic,<sup>16</sup> anti-hypertensive,<sup>17</sup> and neuroprotective effects.<sup>18</sup>

Since detailed investigations of the molecular pathways activated by SAC in endothelial cells are poor, the aim of this study was to evaluate on Bovine Aortic Endothelial cells (BAE-1) the effect of SAC on key elements taking part in vascular health: reactive oxygen species (ROS) intracellular level, H<sub>2</sub>S release, eNOS phosphorylation, and NO production.

Finally, a black garlic extract (BGE) with a high content of SAC was produced, and, together with the chemical characterization, the efficacy of this product was evaluated on BAE-1 cells by assessing H<sub>2</sub>S release in comparison to the treatment with the only standard purified molecule.

## Materials and methods

### Materials

Unless otherwise specified, materials were obtained from Sigma Aldrich (Sigma-Aldrich, Saint Louis, MO, USA). Plastic and reagents for cell cultures were from Euroclone (Euroclone s.p.a., Pero, Italy). Antibodies for immunoblotting experiments were obtained from BD (BD Biosciences, Franklin Lakes, New Jersey, USA) for monoclonal anti-eNOS (Code 610296), Thermo Fisher Scientific (Thermo Fisher Scientific, Waltham, MA, USA) for polyclonal anti-p-eNOS (Code 36-9100), and Sigma-Aldrich for monoclonal anti-β-actin (Code A5316); horseradish peroxidase-conjugated secondary antibodies were from Thermo Fisher Scientific (anti-mouse code: 31430; anti-rabbit code: SA00001-2). S-Allyl-cysteine (SAC) standard was purchased from TCI Europe chemicals (Zwijndrecht, Belgium); S-1-propenyl cysteine (S1PC), γ-Glutamyl-S-1-propenyl cysteine (GS1PC) and γ-Glutamyl-S-1-allyl cysteine (GSAC) were purchased from Medchemtronica (Sollentuna, Sweden). The Black Garlic Extract was produced by the company Biosfered S.r.l. (Turin, Italy) and commercialized as a food supplement ingredient with the brand name *SalliCys*®. Black garlic was prepared based on Choi *et al.*<sup>19</sup> Unpeeled raw garlic heads were incubated in a thermohygrostatic chamber between 60 and

85 °C at high humidity. During the aging process, raw garlic developed a darker color. The aging was stopped when garlic turned completely black. The ground black garlic was extracted by hydroalcoholic solution at room temperature and the supernatant was collected. Ethanol was then removed by vacuum evaporation before use.

### Cell culture

Bovine aortic endothelial cells (BAE-1) were obtained from the European Collection of Authenticated Cell Cultures (ECACC, Salisbury, UK). Cells were maintained in DMEM supplemented with 10% heat-inactivated fetal calf serum (FCS), 50 µg ml<sup>-1</sup> gentamicin, and 2 mM glutamine, in a humidified atmosphere of 5% CO<sub>2</sub> in air. Cells were used at passage 2–6.

To perform the experiments, FCS was not removed as previously done.<sup>20–22</sup>

For fluorescent microscopy experiments on live cells, BAE-1 were plated in DMEM + 10% FCS on uncoated glass bottom dishes, 35 mm diameter (Ibidi, Martinsried, Germany), at a density of 10 000 cells per cm<sup>2</sup> and maintained at 37 °C. After 24 h, cells were loaded with the appropriate probe and stimulated as planned.

### Cell viability assay

Cellular viability was studied by means of crystal violet staining since MTT or similar assays could not be used due to chemical interference of reducing substances in the cellular medium (sulfhydryl-containing compounds such as SAC) with tetrazolium salts.<sup>23</sup> BAE-1 cells were plated in 96-well plates in DMEM + 10% FCS at a density of 10 000 cell per cm<sup>2</sup> (3300 cells per well). Two days later, the medium was replaced with DMEM + 10% FCS, either alone (control condition) or supplemented with SAC at different concentrations (10 µM, 100 µM, 500 µM, 1 mM, 10 mM), 6 wells for each condition. After 4 or 24 h, the effect on cell growth was estimated by staining with crystal violet: cells were fixed in 2.5% glutaraldehyde in PBS for 20 min, then stained with crystal violet (0.1% in 20% methanol); plates were let dry, then the dye was solubilized in acetic acid (10%, v/v) and absorbance read at 595 nm in a microplate reader (FilterMax F5™ Multi-Mode, Molecular Devices, Sunnyvale, CA, USA). Data were expressed as percentages of Abs referred to the control condition; percentage values were then summarized and expressed as mean ± s.e.m.

### H<sub>2</sub>S release

BAE-1 cells, grown on glass bottom dishes, were loaded with 1 µM SF7-AM probe (Cayman Chemical, Ann Arbor, Michigan, USA), for 30 min in the dark. After incubation with the probe, cells were washed two times with phosphate buffered saline (PBS), containing Ca<sup>2+</sup> and Mg<sup>2+</sup>, and then treated with 100 µM sodium hydrosulphide (NaHS) as a positive control or 100 µM SAC, in PBS, for 30 min. Then living cells were washed two times with PBS and the fluorescence was acquired with a fluorescence inverted microscope (Olympus IX70) at 488 nm with a 50× Uplan FI oil-immersion objective. Fluorescence intensity was evaluated in 15 random fields for each condition



through the definition of the Regions Of Interest (ROIs) using the software ImageJ (Rasband, W. S., ImageJ, U. S. National Institutes of Health, Bethesda, Maryland, USA; <https://imagej.nih.gov/ij/>) and expressed in percentage as mean value of the resulting fluorescence for each condition compared to control of three independent experiments  $\pm$  s.e.m.

### Reactive oxygen species (ROS)

BAE-1 cells, grown on glass bottom dishes, were pretreated with 20  $\mu$ M menadione (as a positive control) for 1 h according to Warren *et al.*,<sup>24</sup> or 100  $\mu$ M SAC for 4 h or SAC in combination with menadione; the cells were loaded with 5  $\mu$ M CellROX® green probe (Thermo Fisher Scientific) for the last 30 min in the dark. Then living cells were washed two times with PBS and the fluorescence was acquired with a fluorescence inverted microscope (Olympus IX70) at 488 nm with a 50 $\times$  Uplan FI oil-immersion objective. Fluorescence intensity was evaluated in 15 random fields for each condition through the definition of the ROIs using the software ImageJ and expressed in percentage as the mean value of the resulting fluorescence for each condition compared to control of three independent experiments  $\pm$  s.e.m.

### NO release

BAE-1 cells grown on glass bottom dishes were loaded with 5  $\mu$ M DAR4M-AM probe (Calbiochem), for 30 min in the dark. After incubation with the probe, cells were washed two times with PBS, and then treated in PBS with 100  $\mu$ M ATP as a positive control, for 5 min, or 100  $\mu$ M SAC, for 30 min. Then living cells were washed two times with PBS and the fluorescence was acquired with a fluorescence inverted microscope (Olympus IX70) at 568 nm with a 50 $\times$  Uplan FI oil-immersion objective. Fluorescence intensity was evaluated in 15 random fields for each condition through the definition of the ROIs using the software ImageJ and expressed in percentage as the mean value of the resulting fluorescence for each condition compared to control of three independent experiments  $\pm$  s.e.m.

### Immunoblotting

BAE-1 cells were seeded on plastic dishes, 20 cm<sup>2</sup> of the growth area, at a density of 10 000 cells per cm<sup>2</sup>, in 10% FCS DMEM, and incubated at 37 °C for 48 h. Cells were then treated with 100  $\mu$ M ATP for 5 min as a positive control or with 100  $\mu$ M SAC, for 30 min or 4 h. Cells were lysed in 200  $\mu$ L RIPA lysis buffer (ThermoFisher Scientific) containing phosphatase inhibitor cocktail (PhosSTOP, Roche, Mannheim, Germany), forced through a 1 mL syringe needle and centrifuged at 10 000 rpm for 5 min at 4 °C. Proteins (20  $\mu$ g per lane) were resolved on 8% SDS-PAGE, transferred to a polyvinylidene fluoride membrane (PVDF, Thermo Fisher Scientific) in cold transfer buffer (25 mM Tris pH 8.3, 192 mM glycine, 0.1% SDS, 20% methanol) and blocked for 1 h at 37 °C in TBST (10 mM Tris-HCl, 0.1 M NaCl, 0.1% Tween 20, pH 7.5) plus 5% non-fat dry milk. Blots were incubated overnight at 4 °C with primary antibodies (1 : 500 monoclonal anti-eNOS; 1 : 250

polyclonal anti-*p*-eNOS; 1 : 2000 monoclonal anti- $\beta$  actin). Membranes were then washed three times with TBST and incubated for 1 h at room temperature with secondary antibodies (anti-mouse, 1 : 20 000, for monoclonal antibodies; anti-rabbit, 1 : 10 000, for *p*-eNOS) followed by a second set of three washes with TBST. Bands were visualised by chemiluminescence with Western Lightning Plus-ECL (PerkinElmer, Waltham, MA, USA). Protein levels were determined using the software ImageJ; for each condition ratio of *p*-eNOS/eNOS was evaluated, then normalized toward positive control; results of  $n = 3$  independent experiments were averaged and expressed in percentage as mean  $\pm$  s.e.m. Aspecific staining of secondary antibodies was checked; comparison of  $\beta$  actin intensity ensured equal protein loading.

### HPLC-MRM quantitative analysis of sulfur-containing compounds

For the analysis, 100  $\mu$ L of the liquid extract were weighed and mixed with 1 mL of the initial solvent of the chromatographic run (0.1% formic acid in acetonitrile/0.1% formic acid in water 5 : 95). The resulting solution was then diluted 20 folds and filtered with a 0.22  $\mu$ m PTFE syringe filter. The concentration levels for the calibration curve were prepared in the initial solvent of the chromatographic run as well. The quantitative analysis of SAC, S1PC, GSAC, G1SPC was performed with a HPLC-triple quadrupole MS instrument LCMS8045 by Shimadzu (Japan). An organic gradient of B (acetonitrile 0.1% formic acid) in A (water with 0.1% formic acid) was applied on a Luna C18(2) 150  $\times$  3 mm, 3  $\mu$ m, 100 Å HPLC column (Phenomenex). The gradient method was set as follows: 5% B for the first 2 minutes, 7 minutes 40% B; from the 8th to 9th minute B was kept at 100%, from 9.30 to 14.30 the column was re-conditioned (5% solvent B). Injection volume was 5  $\mu$ L. Column oven was kept at 40 °C. The MS instrument source parameters were: Source: ESI, Nebulizing gas flow (N2): 3 L min<sup>-1</sup>, DL temperature: 250 °C, heat block temperature: 400 °C, drying gas flow (N2): 10 L min<sup>-1</sup>, capillary voltage: 4 kV, positive ion mode. The mass spectrometer was operated in MRM analysis mode using the following transitions: SAC and S1PC: 162.0 > 145.0 as quantitative ions and 162.0 > 73.05, 162 > 41.15 as qualitatives; GSAC and GS1PC: 290 > 162.1 as quantitative and 290 > 145, 290 > 250 as qualitative transitions. Dwell time was set to obtain a total cycle time of 300 ms.

### Statistical analysis

Data are presented as mean  $\pm$  s.e.m. All data were analyzed with ANOVA followed by Bonferroni's multiple comparisons for *post hoc* tests. Differences with  $p < 0.05$  were considered statistically significant.

## Results

### SAC does not affect BAE-1 endothelial cells viability

First aim of this study was to evaluate the effect of SAC on cellular viability. Cells were plated in 96-well plates and treated



with different concentrations of SAC (10  $\mu$ M, 100  $\mu$ M, 500  $\mu$ M, 1 mM, 10 mM). The staining with crystal violet was performed after 4 h or 24 h of treatment. As shown in Fig. 1, both the acute (4 h) and the chronic (24 h) exposure did not significantly affect cellular viability, even at the highest doses.

### SAC enhances hydrogen sulfide release acting as an organic donor

Given that SAC has been the subject of this research on endothelial cells because of its role as an H<sub>2</sub>S donor, a key point of

the study was to verify the actual H<sub>2</sub>S increase in SAC-treated BAE-1 cells. These measurements were performed with the specific fluorescent H<sub>2</sub>S-probe SF7-AM with fluorescence microscopy. The SF7-AM loaded cells were treated with 100  $\mu$ M NaHS as a positive control or 100  $\mu$ M SAC for 30 min. As expected, a significant increase in fluorescence was observed in NaHS-treated cells; furthermore, this increase was significantly detected even in SAC-treated cells, in a comparable way to the positive control (Fig. 2). This result confirmed that SAC acts as an organic donor of H<sub>2</sub>S in our cellular model.

### SAC has an antioxidant activity on menadione-treated cells

As in our model SAC confirmed its noticeable property of H<sub>2</sub>S donor, following experiments were focused on verifying its capacity in inducing the well-known H<sub>2</sub>S-dependent cellular protective pathways. Among these, we started with the antioxidant mechanism.

To evaluate the antioxidant activity of SAC, we performed experiments in fluorescence microscopy, using the CellROX® green fluorescent probe. BAE-1 cells were pretreated with 20  $\mu$ M menadione (MEN, positive control of oxidative stress) for 1 h or 100  $\mu$ M SAC for 4 h alone or in combination with MEN and then labeled with 5  $\mu$ M CellROX® green probe for the last 30 min in the dark. As shown in Fig. 3, SAC did not increase the production of reactive oxygen species (ROS), while the stressor MEN induced an increment of fluorescence intensity as expected, meaning a rise of ROS. However, in cells treated with MEN in combination with SAC, fluorescence was reduced compared to the only MEN treatment. This result confirmed the SAC antioxidant activity in the presence of an oxidative stressor.

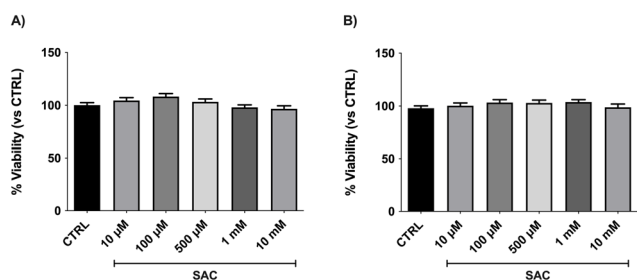


**Fig. 1** SAC does not affect BAE-1 cellular viability. Cells were treated with different concentrations of SAC (10  $\mu$ M, 100  $\mu$ M, 500  $\mu$ M, 1 mM, 10 mM) for 4 h (A) or 24 h (B). Data in percentage referred to the control condition are represented as mean  $\pm$  sem. Values of  $n = 3$  independent experiments for graph 1A were as follow: CTRL: 100.17  $\pm$  2.36; SAC 10  $\mu$ M: 104.46  $\pm$  2.68; SAC 100  $\mu$ M: 108.34  $\pm$  2.86; SAC 500  $\mu$ M: 103.33  $\pm$  2.69; SAC 1 mM: 98.11  $\pm$  2.35; SAC 10 mM: 96.72  $\pm$  2.84. While values of  $n = 3$  independent experiments for graph 1B were as follow: CTRL: 97.99  $\pm$  2.26; SAC 10  $\mu$ M: 100.27  $\pm$  2.64; SAC 100  $\mu$ M: 103.32  $\pm$  2.80; SAC 500  $\mu$ M: 102.88  $\pm$  2.84; SAC 1 mM: 103.86  $\pm$  2.24; SAC 10 mM: 98.78  $\pm$  3.12.

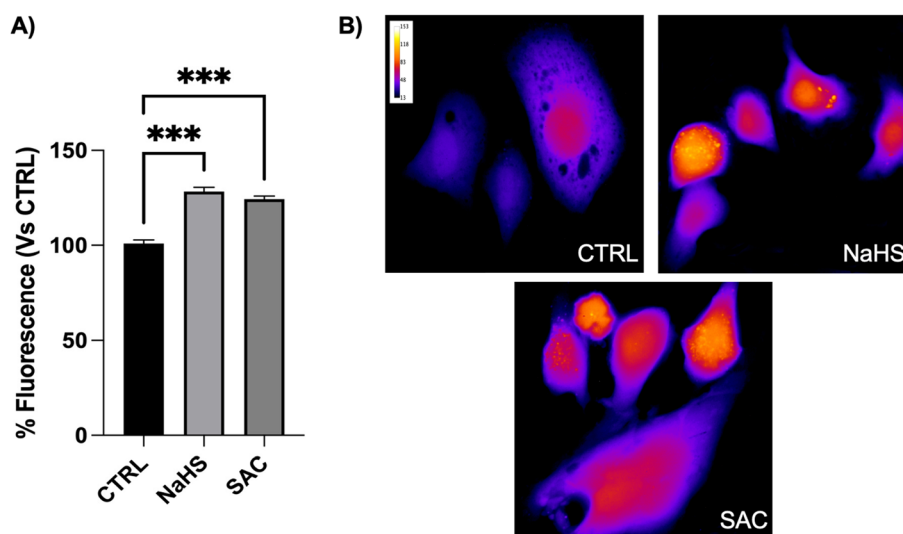


**Fig. 2** SAC enhances H<sub>2</sub>S release on BAE-1 endothelial cells. (A) Bar graph summarizing the significant fluorescence increment after the treatment both with 100  $\mu$ M NaHS and 100  $\mu$ M SAC, in comparison to the control. No significant differences were observed between SAC and NaHS treatment. Data in percentage referred to the control condition are represented as mean  $\pm$  sem, \*\*\* $p < 0.001$ . Values of  $n = 3$  independent experiments were as follow: CTRL: 100.99  $\pm$  1.87,  $n$  cells = 141; NaHS 100  $\mu$ M: 128.34  $\pm$  2.18,  $n$  cells = 146; SAC 100  $\mu$ M: 124.26  $\pm$  1.70,  $n$  cells = 184. (B) Representative fluorescent images (50 $\times$ ) of cells incubated with SF7-AM probe for 30 min in the dark. Images are presented in pseudocolor (LUT = fire) to better show the fluorescent intensity variations (range 0–153).



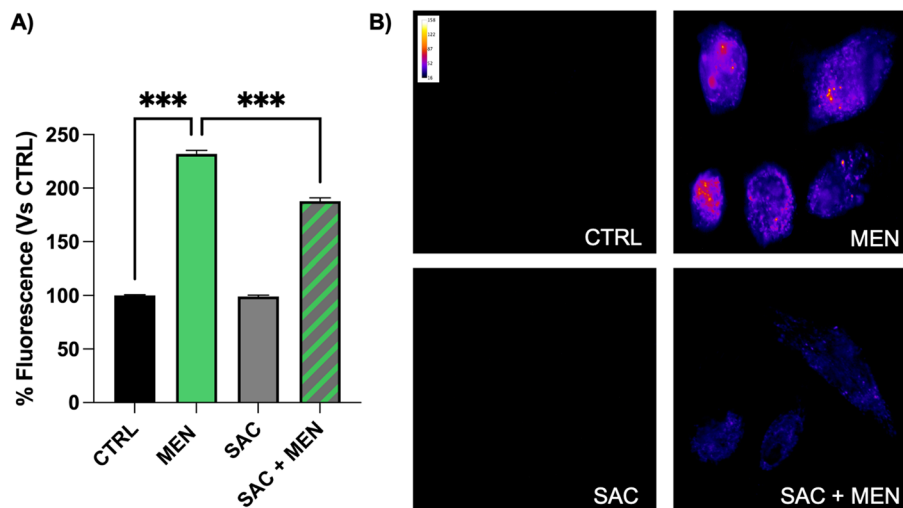


**Fig. 3** SAC decreases ROS production in BAE-1 menadione-treated cells. (A) Bar graph summarizing the effect on ROS production of the pretreatment with 20  $\mu\text{M}$  MEN for 1 h or 100  $\mu\text{M}$  SAC for 4 h or SAC in combination with menadione, in comparison to the control. Data in percentage referred to the control condition are represented as mean  $\pm$  sem, \*\*\* $p$  < 0.001. Values of  $n$  = 3 independent experiments were as follow: CTRL:  $100.00 \pm 0.77$ ,  $n$  cells = 134; MEN 20  $\mu\text{M}$ :  $231.99 \pm 3.36$ ,  $n$  cells = 149; SAC 100  $\mu\text{M}$ :  $98.94 \pm 1.21$ ,  $n$  cells = 130; SAC 100  $\mu\text{M}$  + MEN 20  $\mu\text{M}$ :  $187.91 \pm 2.93$ ,  $n$  cells = 147. (B) Representative fluorescent images (50x) of CellROX® green loaded cells for 30 min in the dark. Images are presented in pseudocolor (LUT = fire) to better show the fluorescence intensity variations (range 0–158).

### SAC improves Endothelial Nitric Oxide Synthase (eNOS) phosphorylation

Previous studies demonstrated that the counteracting effect of  $\text{H}_2\text{S}$  on oxidative stress takes part in the modulation of nitric oxide release, in particular by improving eNOS coupling and phosphorylation.<sup>25</sup> To assign this further protective mechanism to SAC, we performed western blot analysis testing if SAC impacted nitric oxide synthase phosphorylation. Cells were treated with 100  $\mu\text{M}$  ATP for 5 min as a positive control or with 100  $\mu\text{M}$  SAC, for 30 min or 4 h. As represented in Fig. 4, ATP enhanced the nitric oxide phosphorylation as expected. Interestingly, even the SAC treatment both for 30 min and 4 h increased the eNOS phosphorylation in a significant way com-

pared to the control (untreated), thus suggesting a possible implication of SAC in the enhancement of NO release.

### SAC increases nitric oxide release

To demonstrate the involvement of SAC in increasing nitric oxide (NO) release following eNOS phosphorylation, experiments in fluorescence microscopy with the NO probe DAR4M-AM were performed. Cells were first incubated with 5  $\mu\text{M}$  DAR4M-AM probe for 30 min in the dark and then treated with 100  $\mu\text{M}$  ATP or 100  $\mu\text{M}$  SAC, respectively for 5 and 30 min. As shown in Fig. 5, the increased fluorescence intensity after ATP stimulation, which was used as a positive

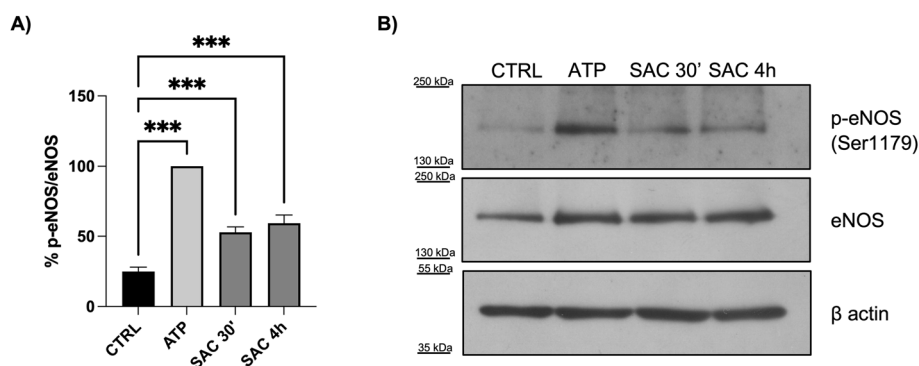


**Fig. 4** SAC positively impacts eNOS phosphorylation in the BAE-1 cell line. (A) Bar graph summarizing the  $p$ -eNOS/eNOS ratio normalized toward positive control (ATP), after treatment with 100  $\mu\text{M}$  ATP (5 min) and 100  $\mu\text{M}$  SAC (30 min and 4 h). Data in percentage are represented as mean  $\pm$  sem, \*\*\* $p$  < 0.001. Values of  $n$  = 3 independent experiments were as follow: CTRL:  $24.76 \pm 3.22$ ; ATP 100  $\mu\text{M}$ :  $100.00 \pm 0.00$ ; SAC 100  $\mu\text{M}$  30 min:  $52.76 \pm 3.92$ ; SAC 100  $\mu\text{M}$  4 h:  $52.76 \pm 5.97$ . (B) Representative western blot experiment showing the effect of ATP and SAC on eNOS phosphorylation. Comparison of  $\beta$  actin intensity ensured equal protein loading.



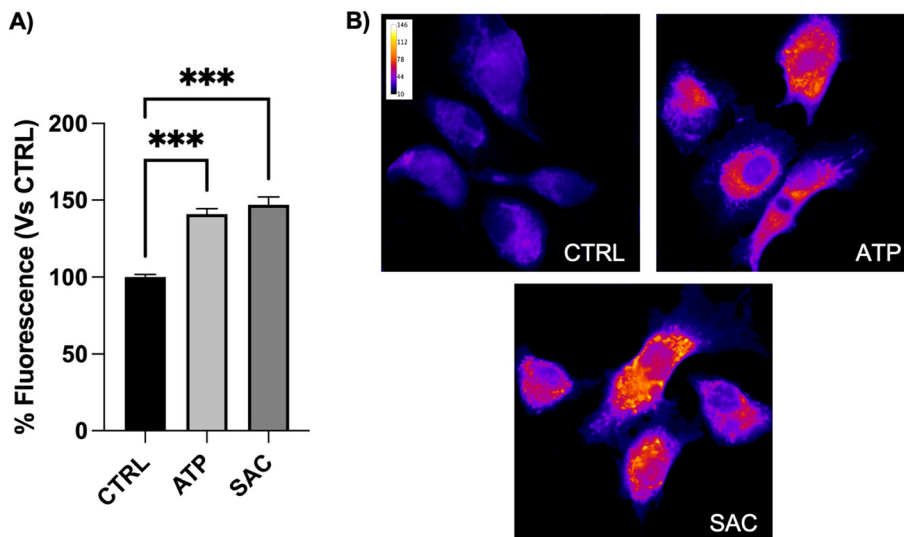


**Fig. 5** SAC enhances the NO release in BAE-1 cells. (A) Bar graph summarizing the fluorescence increment after the stimulation both with 100  $\mu$ M ATP and 100  $\mu$ M SAC, in comparison to the control. No significant differences were observed between SAC and ATP treatment. Data in percentage referred to the control condition are represented as mean  $\pm$  sem, \*\*\* $p$  < 0.001. Values of  $n$  = 3 independent experiments were as follow: CTRL: 100.00  $\pm$  1.77,  $n$  cells = 211; ATP 100  $\mu$ M: 141.03  $\pm$  3.46,  $n$  cells = 146; SAC 100  $\mu$ M: 144.11  $\pm$  5.14,  $n$  cells = 140. (B) Representative fluorescent images (50 $\times$ ) of cells incubated with DAR4M-AM probe for 30 min in the dark. Images are presented in pseudocolor (LUT = fire) to better show the fluorescence intensity variations (range 0–146).

control, was similar to SAC treatment. These results demonstrated the role of SAC in improving NO release in BAE-1 cells.

#### HPLC-MRM method development and application for the quantitation of S-compounds in BGE and pilot process optimization

The previously observed biological effects of SAC could be translated to black garlic, where SAC and other sulfur-containing amino acids have been shown to be highly concentrated with respect to fresh garlic and represent the main antioxidant compounds.<sup>26</sup> In this context, black garlic extract-based formulas represent appealing tools for a nutraceutical approach to the prevention of endothelial dysfunction. To extend our results on SAC in this more food-related field, we moved to the chemical characterization and biological testing on BAE-1 cells of a black garlic extract kindly provided by Biosfered S.r.l. (Turin, Italy). To characterize the S-compounds profile in the black garlic extract (BGE), we developed a fast, simple, and sensitive HPLC-MRM MS method.

For each molecule we investigated three different MRM events; for the isomeric nature of those chemical compounds (SAC is an isomer of S1PC and GSAC is isomeric to GS1PC) the evaluation of the relative abundance of the fragments, together with the elution order is mandatory to avoid their misidentification. The highest-abundant fragment was chosen as the quantifier ion. Once developed and optimized, the method was validated according to ICH guidelines.

The described validated method was used to accurately dose the S-containing compounds SAC, S1PC, GSAC, and GS1PC for the *in vitro* experiments and to monitor their formation yield during the controlled garlic aging process. The

fermentation method which starts with the garlic bulb and leads to the final BGE requires a strict monitoring of the S-compounds abundance profile to trace their formation kinetics and the best moment to stop the aging process. For this study, we developed a BGE extract with a standardized content of S-compounds comparable to the final food-grade ingredient administrable to the cell cultures by dilution with their growth media. The liquid extract showed this profile of S-compounds abundance: SAC: 2.95 mM, S1PC: 0.51 mM, GSAC: 2.8 mM, and GSPC: 0.42 mM (Fig. 6). For the purpose of our experiment, the cell medium solution was prepared to contain a standardized concentration of SAC (100  $\mu$ M) in order to reflect the concentration of SAC used in the experiments with the standard pure molecule.

#### The black garlic extract enriched in SAC improves hydrogen sulfide levels in endothelial cells

First, to test the BGE effect on cellular viability, cells were plated in 96-well plates and treated with 100  $\mu$ M SAC or 100  $\mu$ M BGE for 1 h, followed by the crystal violet staining. As shown in Fig. 7A, 100  $\mu$ M SAC does not affect cellular viability (as already demonstrated in Fig. 1) as well as the treatment with 100  $\mu$ M BGE. Then, to verify if BGE could enhance H<sub>2</sub>S levels in a similar way to the standard, experiments with SF7-AM loaded cells were performed. Cells were treated with 100  $\mu$ M NaHS or 100  $\mu$ M SAC or 100  $\mu$ M BGE. As previously described, there is a significant increase in fluorescence intensity when cells were stimulated with NaHS and SAC, but even with BGE treatment, the fluorescence is higher in a significant way in comparison to the control condition (Fig. 7B and C), thus suggesting that BGE enhances H<sub>2</sub>S levels in our cellular model.



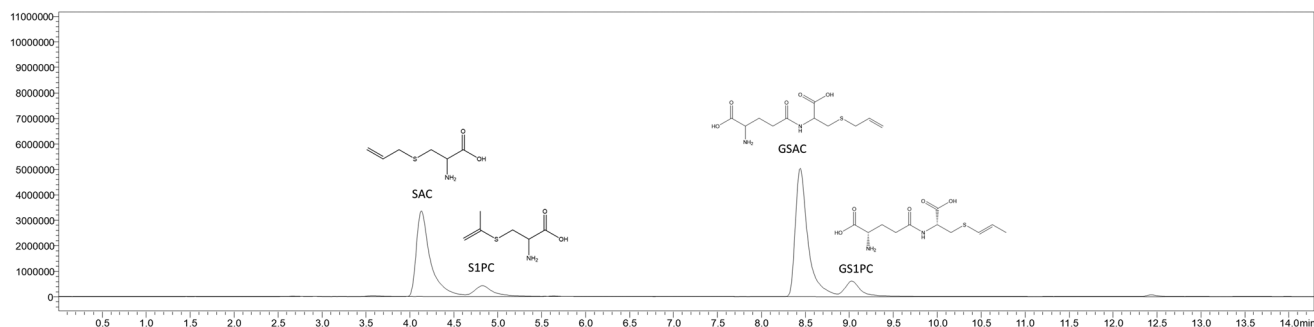


Fig. 6 Chromatographic separation of the *S*-compounds in the liquid sample of BGE used for cells treatments. For each peak, the compound name, as well as its structural formula, is presented.

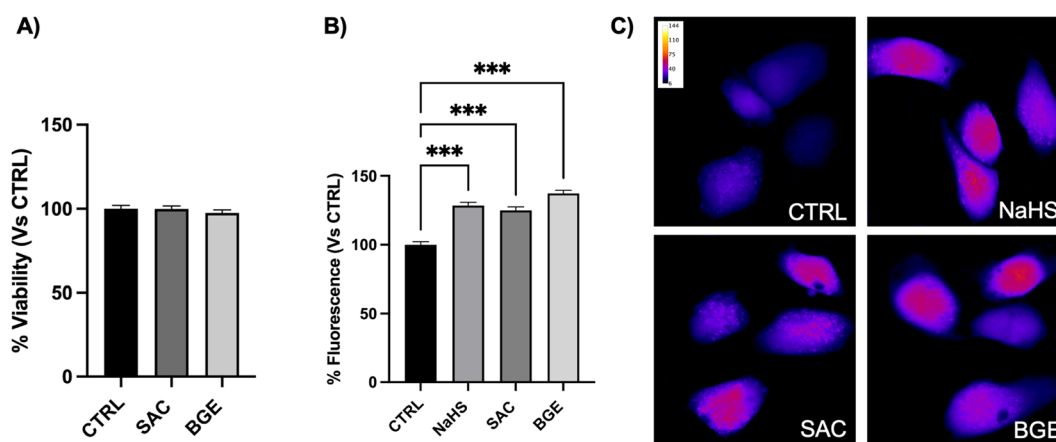


Fig. 7 BGE improves  $\text{H}_2\text{S}$  release on BAE-1 cells in a similar way to the standard. (A) 100  $\mu\text{M}$  BGE does not affect BAE-1 viability after 1 h treatment. Data in percentage referred to the control condition are represented as mean  $\pm$  sem. Values of  $n = 3$  independent experiments were as follow: CTRL:  $100.08 \pm 1.92$ ; SAC 100  $\mu\text{M}$ :  $99.99 \pm 1.70$ ; BGE 100  $\mu\text{M}$ :  $97.61 \pm 1.68$ . (B) Bar graph summarizing the significant fluorescent increment after the treatment with 100  $\mu\text{M}$  NaHS, 100  $\mu\text{M}$  SAC, and 100  $\mu\text{M}$  BGE, in comparison to the control. Data in percentage referred to the control condition are represented as mean  $\pm$  sem,  $***p < 0.001$ . Values of  $n = 3$  independent experiments were as follow: CTRL:  $100.00 \pm 2.15$ ,  $n$  cells = 174; NaHS 100  $\mu\text{M}$ :  $128.53 \pm 2.39$ ,  $n$  cells = 172; SAC 100  $\mu\text{M}$ :  $125.07 \pm 2.53$ ,  $n$  cells = 171; BGE 100  $\mu\text{M}$ :  $137.48 \pm 2.22$ ,  $n$  cells = 173. (C) Representative fluorescent images (50x) of cells incubated with SF7-AM probe for 30 min in the dark. Images are presented in pseudocolor (LUT = fire) to better show the fluorescence intensity variations (range 0–144).

## Discussion

This study is focused on two main goals: first, to demonstrate in BAE-1 cells that the sulfur-containing amino acid *S*-allyl cysteine (SAC) is an effective intracellular source of  $\text{H}_2\text{S}$  and is able to improve nitric oxide release; second, to demonstrate the  $\text{H}_2\text{S}$  donor capabilities on BAE-1 cells of the chemically characterized commercial black garlic extract (BGE) (*SalliCys*®). The ‘polar star’ of these items is the gasotransmitter  $\text{H}_2\text{S}$ , which we showed was released from both SAC and BGE and to whom the protective mechanisms activated by SAC on endothelial cells are ascribed.

The fundamental role of  $\text{H}_2\text{S}$  in vascular physiology has been indeed clearly evidenced,<sup>27</sup> and the beneficial effects of its supplementation to improve endothelial function have been proven both in experimental models and in clinical investigations.<sup>28</sup>

Several methods of  $\text{H}_2\text{S}$  delivery and supplementation have been tested, the main classes of  $\text{H}_2\text{S}$  pro-drugs being hydrolysis-based donors, plant-derived natural donors, and controlled-release donors.<sup>29</sup> Among these molecules, plant-derived donors, mainly organic polysulfides from garlic, received great attention in the last decade for their potential use as nutraceuticals, in particular for the prevention of cardiovascular disorders. SAC belongs to the organic polysulfide family and has been studied for many years for its biological activities,<sup>30</sup> particularly in counteracting endothelial dysfunction through  $\text{H}_2\text{S}$  release.<sup>31</sup>

However, reports directly showing  $\text{H}_2\text{S}$  intracellular increase after treatment with SAC are still lacking. To prove this  $\text{H}_2\text{S}$  rise in BAE-1 cells, we performed fluorescence measurements with the  $\text{H}_2\text{S}$  probe SF7-AM. Results are shown in Fig. 2 and highlight a significant increase in intracellular  $\text{H}_2\text{S}$  levels in both NaHS (positive control) and SAC-treated cells. To our knowledge, this is the first evidence in a cellular model of the



SAC-induced H<sub>2</sub>S rise. The H<sub>2</sub>S intracellular detection with fluorescent probes has been previously shown in several endothelial cell models, as in NaHS-stimulated<sup>32</sup> or VEGF-stimulated HUVEC,<sup>33</sup> and here we showed this rise after treatment of endothelial cells with the organic and natural H<sub>2</sub>S donor SAC. This evidence establishes a solid ground to support the subsequent experiments focused on the biological effects of SAC on BAE-1 cells. Among these, we first investigated and confirmed the antioxidant mechanism (Fig. 3), showing a significant reduction of menadione-induced intracellular ROS in BAE-1 cells preincubated with SAC. The antioxidant activity of SAC on endothelial cells was first highlighted by Ide *et al.*<sup>34</sup> and is dependent on the multifaceted antioxidant role of H<sub>2</sub>S: it indeed reduces ROS levels by both direct mechanisms (ROS scavenging, increase in SOD activity) and indirect pathways (increase in non-enzymatic antioxidant systems, increase in Nrf2-dependent expression of antioxidant enzymes).<sup>35</sup>

In agreement with the results on ROS, we then underlined a positive modulatory role of SAC on eNOS activity and thus on the endothelial function. As shown in Fig. 4 and 5, SAC enhances the eNOS phosphorylation and the nitric oxide intracellular level in BAE-1. These data are aligned with previous studies highlighting the strict interconnection between H<sub>2</sub>S and NO, because of the multiple mechanisms by which H<sub>2</sub>S positively affects eNOS activity.<sup>27</sup> Thus, we confirmed these mechanisms also in SAC-treated endothelial cells, strengthening the interest in the molecule as a natural compound improving nitric oxide-mediated vascular functions. The choice to test 100 μM SAC was grounded on the evidence that this concentration strictly corresponds to the plasmatic level of SAC (15,2 μg ml<sup>-1</sup>) detected in the plasma of rats subjected to oral administration of 25 mg kg<sup>-1</sup> SAC.<sup>36</sup> Moreover, this oral dosage corresponds to that employed in several *in vivo* studies on rats, aimed to highlight SAC-dependent cardioprotective effects;<sup>31</sup> giving the high bioavailability of the molecule, this dosage could lead to the same plasmatic concentration of 15,2 μg ml<sup>-1</sup>. SAC pharmacokinetic has been indeed investigated by Lee *et al.*<sup>36</sup> and by Amano *et al.* in rats;<sup>37</sup> these studies showed a very high bioavailability of the molecule, that was respectively 96% (with 25 mg kg<sup>-1</sup> SAC o.a.) and (5 mg kg<sup>-1</sup> o.a.). We could speculate a similar bioavailability in humans, even if specific data are still missing. We then decided to go forward by achieving the *in vitro* characterisation of the functional effects of the BGE, in order to understand whether the addition of the matrix complexity was affecting results obtained with SAC. The choice of black garlic comes from its higher content in SAC, which, as reported by several studies, varies from three to six times with respect to fresh garlic.<sup>26</sup> To fulfill this purpose, we first decided to quantitate the S-compounds present in the BGE to standardize their abundance in the aliquot which was administered to the cells. The knowledge of the accurate quantitation value is essential to calculate the dose–response relationship and accordingly, to formulate a proper dosage. The scientific literature reports several methods for the quantitation of S-compounds: an application for the S-allyl cysteine quantitative study has been

developed with a HPLC-FLD and HPLC-UV detector; in this case, for the poor response of SAC with spectrophotometric detectors a derivatization step is strongly required.<sup>38–40</sup> The use of a MS detector overcomes this limitation and allows the analysis to reach a higher sensitivity; an interesting HPLC-MS method was validated for the quantitation of SAC in heated garlic juice with similar conditions to ours;<sup>41</sup> the paper presents an interesting comparison between UV and MS detector and highlights the sensitivity differences between the two techniques. For our method, the optimal chromatographic conditions were found using a Luna C18 (2) column with an organic gradient of 0.1% formic acid in ACN starting from 5% in 0.1% formic acid in water. An initial isocratic step with the initial solvent condition was revealed as a successful strategy for the separation of the hydrophilic isomeric compounds SAC and S1PC without co-elutions as well as the later-eluting GSAC and GS1PC in a total of 14 minutes. After quantifying the S-containing compounds SAC, S1PC, GSAC, and GS1PC in the BGE for their proper dosage on BAE-1 cells, we verified that 100 μM BGE didn't affect cell viability after 1 h of treatment. For times of exposure exceeding 1 h, cells were suffering from osmotic stress caused by the high total sugars content of the extract (382 g kg<sup>-1</sup> – 38.2% w/w, spectrophotometer Anthrone assay data, not shown). Since the BGE doesn't reach the target cells (after oral assumption) in this form, as sugars follow different metabolic pathways after ingestion, the cytotoxicity (for >1 h exposure) and NO release of the whole extract were not representative. Successively, we demonstrated the H<sub>2</sub>S-releasing feature of BGE on cells. As shown in Fig. 7, BGE-treated cells displayed a significant increase in the H<sub>2</sub>S level with respect to control cells, similarly to NaHS and SAC-treated cells. This last experiment represents a smart and original approach to test plant-derived extracts as H<sub>2</sub>S-donors on *in vitro* cellular models; furthermore, it supports the forcefulness of BGE for further investigations and nutraceutical applications.

## Conclusions

In conclusion, our study clearly highlights the beneficial roles of SAC on endothelial health, by demonstrating its features as an antioxidant, H<sub>2</sub>S donor, and NO availability enhancer; moreover, the results showing SAC-induced nitric oxide release and eNOS phosphorylation boost knowledges of its strict relation with the NO-pathway. In addition, by directly showing the intracellular H<sub>2</sub>S rise in SAC and BGE-treated endothelial cells, this study recommends an efficient and useful approach to characterize the vasoprotective H<sub>2</sub>S-dependent functions of bioactive molecules or extracts. Furthermore, the presented profiling of S-compounds paves the way to a more comprehensive characterization of the other compounds present in the BGE through untargeted MS-based metabolomic approaches. This global metabolomic profile of the ingredient, now in progress, will draw a bigger picture of the pool of the bioactive metabolites residing in this unknown yet promising food matrix.



## Conflicts of interest

A. O. and A. P. are employed by Abel Nutraceuticals S.r.l.; A. A. is a student of the Ph.D. Program in Chemical and Material Sciences of the University of Turin (XXXVI cycle) and in apprenticeship at Biosfered S.r.l. The remaining authors declare that the research was conducted in the absence of any commercial or financial relationships that could be construed as a potential conflict of interest. The funders had no role in the design of the study; in the collection, analyses, or interpretation of data; in the writing of the manuscript; or in the decision to publish the results.

## Acknowledgements

We thank Biosfered S.r.l. for kindly providing the Black Garlic Extract (*SalliCys*®).

## References

- 1 S. Godo and H. Shimokawa, Endothelial Functions, *Arterioscler. Thromb. Vasc. Biol.*, 2017, **37**, e108–e114.
- 2 V. Ciccone, S. Genah and L. Morbidelli, Endothelium as a Source and Target of H<sub>2</sub>S to Improve Its Trophism and Function, *Antioxidants*, 2021, **10**, 486.
- 3 P. Poredos, A. V. Poredos and I. Gregoric, Endothelial Dysfunction and Its Clinical Implications, *Angiology*, 2021, **72**, 604–615.
- 4 R. Wang, C. Szabo, F. Ichinose, A. Ahmed, M. Whiteman and A. Papapetropoulos, The role of H<sub>2</sub>S bioavailability in endothelial dysfunction, *Trends Pharmacol. Sci.*, 2015, **36**, 568–578.
- 5 K. M. Casin and J. W. Calvert, Harnessing the Benefits of Endogenous Hydrogen Sulfide to Reduce Cardiovascular Disease, *Antioxidants*, 2021, **10**, 383.
- 6 V. Citi, A. Martelli, E. Gorica, S. Brogi, L. Testai and V. Calderone, Role of hydrogen sulfide in endothelial dysfunction: Pathophysiology and therapeutic approaches, *J. Adv. Res.*, 2021, **27**, 99–113.
- 7 S. Huerta de la Cruz, G. J. Medina-Terol, J. A. Tapia-Martínez, D. L. Silva-Velasco, J. H. Beltran-Ornelas, A. Sánchez-López, M. Sancho and D. Centurión, Hydrogen sulfide as a neuromodulator of the vascular tone, *Eur. J. Pharmacol.*, 2023, **940**, 175455.
- 8 R. Varshney and M. J. Budoff, Garlic and Heart Disease, *J. Nutr.*, 2016, **146**, 416S–421S.
- 9 A. Corvino, F. Frecentese, E. Magli, E. Perissutti, V. Santagada, A. Scognamiglio, G. Caliendo, F. Fiorino and B. Severino, Trends in H<sub>2</sub>S-Donors Chemistry and Their Effects in Cardiovascular Diseases, *Antioxidants*, 2021, **10**, 429.
- 10 A. Shang, S.-Y. Cao, X.-Y. Xu, R.-Y. Gan, G.-Y. Tang, H. Corke, V. Mavumengwana and H.-B. Li, Bioactive Compounds and Biological Functions of Garlic (*Allium sativum* L.), *Foods*, 2019, **8**, 246.
- 11 A. L. Colín-González, S. F. Ali, I. Túnez and A. Santamaría, On the antioxidant, neuroprotective and anti-inflammatory properties of S-allyl cysteine: An update, *Neurochem. Int.*, 2015, **89**, 83–91.
- 12 A. L. Colín-González, R. A. Santana, C. A. Silva-Islas, M. E. Chánez-Cárdenas, A. Santamaría and P. D. Maldonado, The Antioxidant Mechanisms Underlying the Aged Garlic Extract- and S-Allylcysteine-Induced Protection, *Oxid. Med. Cell. Longevity*, 2012, **2012**, 1–16.
- 13 G. Saravanan and P. Ponmurugan, Ameliorative potential of S-allyl cysteine on oxidative stress in STZ induced diabetic rats, *Chem.-Biol. Interact.*, 2011, **189**, 100–106.
- 14 G. Saravanan and P. Ponmurugan, Beneficial Effect of S-allylcysteine (SAC) on Blood Glucose and Pancreatic Antioxidant System in Streptozotocin Diabetic Rats, *Plant Foods Hum. Nutr.*, 2010, **65**, 374–378.
- 15 M. Thomson and M. Ali, Garlic [*Allium sativum*]: A Review of its Potential Use as an Anti-Cancer Agent, *Curr. Cancer Drug Targets*, 2003, **3**, 67–81.
- 16 S. Kodai, S. Takemura, Y. Minamiyama, S. Hai, S. Yamamoto, S. Kubo, Y. Yoshida, E. Niki, S. Okada, K. Hirohashi and S. Suehiro, S-allyl cysteine prevents CCl<sub>4</sub>-induced acute liver injury in rats, *Free Radic. Res.*, 2007, **41**, 489–497.
- 17 J.-M. Kim, N. Chang, W.-K. Kim and H. S. Chun, Dietary S-Allyl-L-cysteine Reduces Mortality with Decreased Incidence of Stroke and Behavioral Changes in Stroke-Prone Spontaneously Hypertensive Rats, *Biosci. Biotechnol. Biochem.*, 2006, **70**, 1969–1971.
- 18 Y. Kosuge, Neuroprotective mechanisms of S-allyl-L-cysteine in neurological disease (Review), *Exp. Ther. Med.*, 2020, **19**, 1565–1569.
- 19 I. S. Choi, H. S. Cha and Y. S. Lee, Physicochemical and antioxidant properties of black garlic, *Molecules*, 2014, **19**, 16811–16823.
- 20 G. Querio, S. Antoniotti, F. Geddo, R. Levi and M. P. Gallo, Trimethylamine N-Oxide (TMAO) Impairs Purinergic Induced Intracellular Calcium Increase and Nitric Oxide Release in Endothelial Cells, *Int. J. Mol. Sci.*, 2022, **23**, 3982.
- 21 G. Querio, S. Antoniotti, F. Foglietta, C. M. Berteau, R. Canaparo, M. P. Gallo and R. Levi, Chamazulene Attenuates ROS Levels in Bovine Aortic Endothelial Cells Exposed to High Glucose Concentrations and Hydrogen Peroxide, *Front. Physiol.*, 2018, **9**, 246.
- 22 S. Fornero, E. Bassino, R. Ramella, C. Gallina, S. K. Mahata, B. Tota, R. Levi, G. Alloatti and M. P. Gallo, Obligatory Role for Endothelial Heparan Sulphate Proteoglycans and Caveolae Internalization in Catestatin-Dependent eNOS Activation, *BioMed Res. Int.*, 2014, **2014**, 1–10.
- 23 E. Scarcello, A. Lambremont, R. Vanbever, P. J. Jacques and D. Lison, Mind your assays: Misleading cytotoxicity with the WST-1 assay in the presence of manganese, *PLoS One*, 2020, **15**, e0231634.



- 24 M. C. Warren, E. A. Bump, D. Medeiros and S. J. Braunhut, Oxidative stress-induced apoptosis of endothelial cells, *Free Radicals Biol. Med.*, 2000, **29**, 537–547.
- 25 A. L. King, D. J. Polhemus, S. Bhushan, H. Otsuka, K. Kondo, C. K. Nicholson, J. M. Bradley, K. N. Islam, J. W. Calvert, Y.-X. Tao, T. R. Dugas, E. E. Kelley, J. W. Elrod, P. L. Huang, R. Wang and D. J. Lefer, Hydrogen sulfide cytoprotective signaling is endothelial nitric oxide synthase-nitric oxide dependent, *Proc. Natl. Acad. Sci. U. S. A.*, 2014, **111**, 3182–3187.
- 26 T. Ahmed and C.-K. Wang, Black Garlic and Its Bioactive Compounds on Human Health Diseases: A Review, *Molecules*, 2021, **26**, 5028.
- 27 G. K. Kolluru, R. E. Shackelford, X. Shen, P. Dominic and C. G. Kevil, Sulfide regulation of cardiovascular function in health and disease, *Nat. Rev. Cardiol.*, 2023, **20**, 109–125.
- 28 E. Magli, E. Perissutti, V. Santagada, G. Caliendo, A. Corvino, G. Esposito, G. Esposito, F. Fiorino, M. Migliaccio, A. Scognamiglio, B. Severino, R. Sparaco and F. Frecentese, H<sub>2</sub>S Donors and Their Use in Medicinal Chemistry, *Biomolecules*, 2021, **11**, 1899.
- 29 Y. Zheng, X. Ji, K. Ji and B. Wang, Hydrogen sulfide pro-drugs—a review, *Acta Pharm. Sin. B*, 2015, **5**, 367–377.
- 30 B. Yudhistira, F. Punthi, J. Lin, A. S. Sulaimana, C. Chang and C. Hsieh, S-Allyl cysteine in garlic (*Allium sativum*): Formation, biofunction, and resistance to food processing for value-added product development, *Compr. Rev. Food Sci. Food Saf.*, 2022, **21**, 2665–2687.
- 31 J. M. Alves-Silva, M. Zuzarte, H. Girão and L. Salgueiro, Natural Products in Cardiovascular Diseases: The Potential of Plants from the Alliioideae Subfamily (Ex-Alliaceae Family) and Their Sulphur-Containing Compounds, *Plants*, 2022, **11**, 1920.
- 32 L. Wu, L. Chen, M. Kou, Y. Dong, W. Deng, L. Ge, H. Bao, Q. Chen and D. Li, The ratiometric fluorescent probes for monitoring the reactive inorganic sulfur species (RISS) signal in the living cell, *Spectrochim. Acta, Part A*, 2020, **231**, 118141.
- 33 V. S. Lin, A. R. Lippert and C. J. Chang, Cell-trappable fluorescent probes for endogenous hydrogen sulfide signaling and imaging H<sub>2</sub>O<sub>2</sub>-dependent H<sub>2</sub>S production, *Proc. Natl. Acad. Sci. U. S. A.*, 2013, **110**, 7131–7135.
- 34 N. Ide and B. H. Lau, Garlic compounds protect vascular endothelial cells from oxidized low density lipoprotein-induced injury, *J. Pharm. Pharmacol.*, 1997, **49**, 908–911.
- 35 J. Liu, F. M. Mesfin, C. E. Hunter, K. R. Olson, W. C. Shelley, J. P. Brokaw, K. Manohar and T. A. Markel, Recent Development of the Molecular and Cellular Mechanisms of Hydrogen Sulfide Gasotransmitter, *Antioxidants*, 2022, **11**, 1788.
- 36 S. Lee, N. I. Chang, M. Yoo, J. H. Choi and D. Shin, Development and Validation of S-Allyl-L-Cysteine in Rat Plasma Using a Mixed-Mode Reversed-Phase and Cation-Exchange LC-ESI-MS/MS Method: Application to Pharmacokinetic Studies, *J. Chromatogr. Sci.*, 2015, **53**, 54–59.
- 37 H. Amano, D. Kazamori and K. Itoh, Pharmacokinetics of S-Allyl-L-cysteine in Rats Is Characterized by High Oral Absorption and Extensive Renal Reabsorption, *J. Nutr.*, 2016, **146**, S456–S459.
- 38 S. E. Bae, S. Y. Cho, Y. D. Won, S. H. Lee and H. J. Park, A comparative study of the different analytical methods for analysis of S-allyl cysteine in black garlic by HPLC, *LWT – Food Sci. Technol.*, 2012, **46**, 532–535.
- 39 S. Hirata, M. Abdelrahman, N. Yamauchi and M. Shigyo, Characteristics of chemical components in genetic resources of garlic *Allium sativum* collected from all over the world, *Genet. Resour. Crop Evol.*, 2016, **63**, 35–45.
- 40 C. Malaphong, A. Tangwanitchakul, S. Boriboon and N. Tangtreamjitmun, A simple and rapid HPLC method for determination of S-allyl-L-cystein and its use in quality control of black garlic samples, *LWT*, 2022, **160**, 113290.
- 41 S. Lee, M. Yoo, S. Kim and D. Shin, Identification and quantification of S-allyl-l-cysteine in heated garlic juice by HPLC with ultraviolet and mass spectrometry detection, *LWT – Food Sci. Technol.*, 2014, **57**, 516–521.

